Band gaps and Brekhovskikh attenuation of laser-generated surface acoustic waves in a patterned thin film structure on silicon

A. A. Maznev*
Department of Applied Physics, Graduate School of Engineering, Hokkaido University, Sapporo 060-8628, Japan
(Received 12 February 2008; revised manuscript received 19 September 2008; published 24 October 2008)

Surface acoustic modes of a periodic array of copper and SiO_2 lines on a silicon substrate are studied using a laser-induced transient grating technique. It is found that the band gap formed inside the Brillouin zone due to "avoided crossing" of Rayleigh and Sezawa modes is much greater than the band gap in the Rayleigh wave dispersion formed at the zone boundary. Another unexpected finding is that a very strong periodicity-induced attenuation is observed above the longitudinal threshold rather than above the transverse threshold.

DOI: 10.1103/PhysRevB.78.155323 PACS number(s): 68.35.Iv, 63.22.Np, 62.65.+k

I. INTRODUCTION

Recent progress in the investigation of phononic crystals[1] stimulated renewed interest in surface acoustic waves (SAWs) in periodic structures. Most studies published to date, both theoretical and experimental, dealt with a homogeneous solid medium having a periodic surface profile.[2–7] Periodic elastic composites have also been considered.[8,9] Recently, structures with the periodicity created by fabricating a patterned thin film on a homogeneous substrate have been attracting increased attention.[10–12] Structures comprised of metal wires embedded in a dielectric film are of particular practical importance due to their ubiquitous role in microelectronics. In recent years, semiconductor industry has been increasingly relying on measurement systems utilizing laser-generated acoustic waves in order to control the fabrication of metal interconnects on silicon chips.[13] Aside from this practical aspect, optoacoustic measurements on metal interconnect structures pose some interesting wave propagation problems.

Antonelli *et al.*[10] used a picosecond pump-probe method to study vibrations of an array of submicron-wide copper lines embedded in a SiO_2 film and identified a number of normal modes up to 10 GHz in frequency. Their technique, however, was limited to nonpropagating vibrational modes corresponding to the zero wave vector. Profunser *et al.*[11] used a different variation of the picosecond pump-probe technique allowing a full two-dimensional mapping of surface acoustic waves propagating from a point source on an array of 2-μm-wide lines. Bloch harmonics and a stopband were observed, but the resolution of the measurement was not sufficient to resolve the details of the band structure.

In this work, surface acoustic modes in a line array structure similar to that of Ref. 11 are studied with a laser-induced transient grating technique also known as impulsive-stimulated thermal scattering.[6,14] This technique is well suited to study surface acoustic modes in periodic structures.[6] On one hand, in contrast to more conventional transmission experiments[7] where transducer and receiver are located outside the structure of interest, the technique permits studying nonpropagating (zero group velocity) and highly attenuated modes. On the other hand, it provides a higher resolution of the acoustic frequency measurements compared to other optical techniques such as Brillouin scattering[3,5] and two-dimensional pump-probe imaging,[11] thus making it possible to study fine details of the band structure.

II. EXPERIMENT

A cross section of the sample is schematically shown in Fig. 1(a). Copper lines are embedded in the 0.8-μm-thick SiO_2 film on a (100) Si wafer. The substrate is 720 μm thick and thus can be considered semi-infinite for the purposes of this study. Copper line width is 1.5 μm and the structure period $d=3$ μm. A very thin (25 nm) Ta diffusion barrier layer separates Cu from Si and SiO_2. The lines are aligned

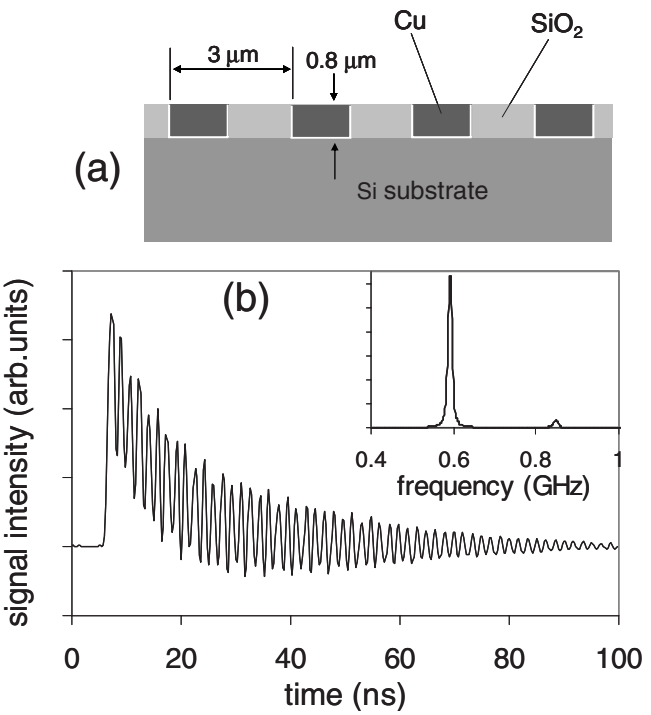

FIG. 1. (a) Cross section of the sample and (b) a typical signal wave form for the SAW propagation direction parallel to Cu lines measured at wave number 0.98 μm^{-1} (acoustic wavelength 6.4 μm). Fast Fourier transform (FFT) spectrum of acoustic oscillations is shown in the inset.

along the ⟨011⟩ axis of Si. The dimensions of the line array pattern are 3×3 mm.

The transient grating setup with optical heterodyne detection[15] has been described in details elsewhere.[16] In short, two excitation pulses derived from a single laser source (pulse duration is 0.5 ns, wavelength is 532 nm, and total energy at the sample is ~1 μJ) are crossed at the sample surface to form a spatially periodic intensity pattern. The period of this excitation grating can be varied within the range 3.9–9.8 μm (wave-number range 0.64–1.6 μm^{-1}). Absorption of the excitation light followed by rapid thermal expansion generates counter-propagating acoustic modes at the wave number defined by the periodicity of the excitation grating. Since the excitation grating is produced by imaging a phase mask on the sample surface,[15,16] the acoustic wave number is known with high precision. To account for a small deviation in the magnification of the imaging optics from the nominal value of 1:1, the system was additionally calibrated by "burning" a permanent grating in a thin Ta film and measuring its period with a microscope versus a NIST-traceable line pattern standard. Thus the estimated error in the wave-number values does not exceed 0.1%. In the discussion below, wave-number values are rounded to two–three significant digits unless a precise number is essential.

Detection of the acoustic waves is performed via diffraction of a quasi-cw probe beam (wavelength is 830 nm and power at the sample is ~100 mW) focused at the center of the excitation pattern. Diffraction signal amplified via optical heterodyning[15] is detected with a fast photodiode and fed to a digital oscilloscope, with the effective bandwidth of the setup being ~1 GHz. The excitation spot size is 300×50 μm (the long dimension along the wave vector of the grating), i.e., much smaller than the dimensions of the line array pattern, and the probe spot size is 50×25 μm.

Measurements were performed in two configurations, with the excitation grating wave vector parallel and perpendicular to the Cu lines. In both cases the acoustic wave vector is along the ⟨011⟩ symmetry direction, therefore only saggitally polarized acoustic waves are excited.

III. RESULTS AND DISCUSSION

A. Propagation parallel to Cu lines

A typical signal wave form for the grating wave vector parallel to the Cu lines is presented in Fig. 1(b). The sharp rise from the zero level indicates a moment when the excitation pulse strikes the sample. Surface displacement amplitude at the signal maximum is in the order of 0.1 nm. High-frequency oscillations are due to surface acoustic modes while the slowly decaying component is the contribution of the "thermal grating" associated with the periodic temperature profile.[14] The decay of the acoustic oscillations is caused mainly by the finite length of the excitation spot, as the counter-propagating SAW wave packets leave the probing area. The Fourier spectrum of the acoustic oscillations reveals the presence of two surface acoustic modes as is not uncommon for film/substrate structures:[14,17] the fundamental and the weak second-order modes, often referred to as Rayleigh and Sezawa waves, respectively.

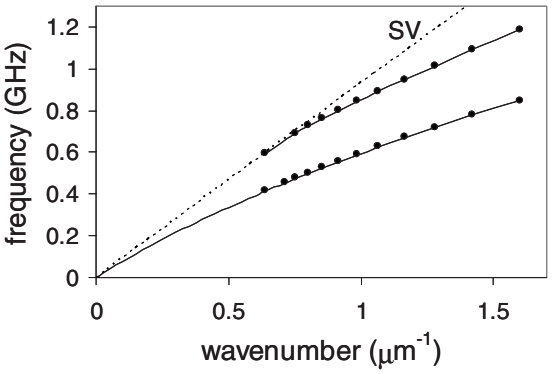

FIG. 2. Measured dispersion curves (solid circles) of surface acoustic modes propagating parallel to Cu lines. Solid lines represent effective-medium calculations. Dotted line corresponds to the vertically polarized bulk transverse wave in Si.

Acoustic dispersion curves presented in Fig. 2 are, again, quite typical for a structure comprising a "slow" film on a "fast" substrate,[17] with the Sezawa mode emerging from under the "cutoff " determined by the velocity of the vertically polarized bulk transverse wave. Figure 2 also shows calculated dispersion curves for a homogeneous layer with effective elastic properties.[18] As the structure period is comparable to the acoustic wavelength, the effective-medium approximation is not expected to be highly accurate. Nevertheless, it yields a surprisingly good agreement with the experimental data.

B. Propagation perpendicular to Cu lines

Measurements with the grating wave vector perpendicular to the lines reveal a different picture. Signal wave forms generally contain three acoustic modes. In the discussion below the modes are referred to as the first, second, and third in the order of increasing frequency.

Figure 3 presents examples of wave forms obtained at wave numbers 0.91 and 1.16 μm^{-1}. One can see that excellent signal-to-noise ratio permits the detection of extremely weak peaks in the spectrum. Despite of a large difference in the wave number, both measurements yield almost the same acoustic frequencies. The reason for this is that the wave numbers are nearly symmetric with respect to the Brillouin-zone boundary of the periodic structure $k_B=\pi/3$ μm^{-1}.

Acoustic dispersion curves are presented in Fig. 4(a). The measurements are indeed symmetric with respect to the Brillouin-zone boundary. Therefore, it is instructive to plot the dispersion curves versus the reduced wave number k_r as it is done in Fig. 4(b). The symmetry, however, only applies to the measured frequencies and not to the signal wave forms. When the wave vector is smaller than k_B the signal is dominated by the first mode, as can be seen from Fig. 3. Beyond the Brillouin-zone boundary the second and then the third mode becomes dominant. The apparent explanation for this behavior is that the mode closest to the original Rayleigh wave at a given wave number is excited most efficiently.

As expected, the dispersion curves shown in Fig. 4 form a band gap at the Brillouin-zone boundary. It should be noted,

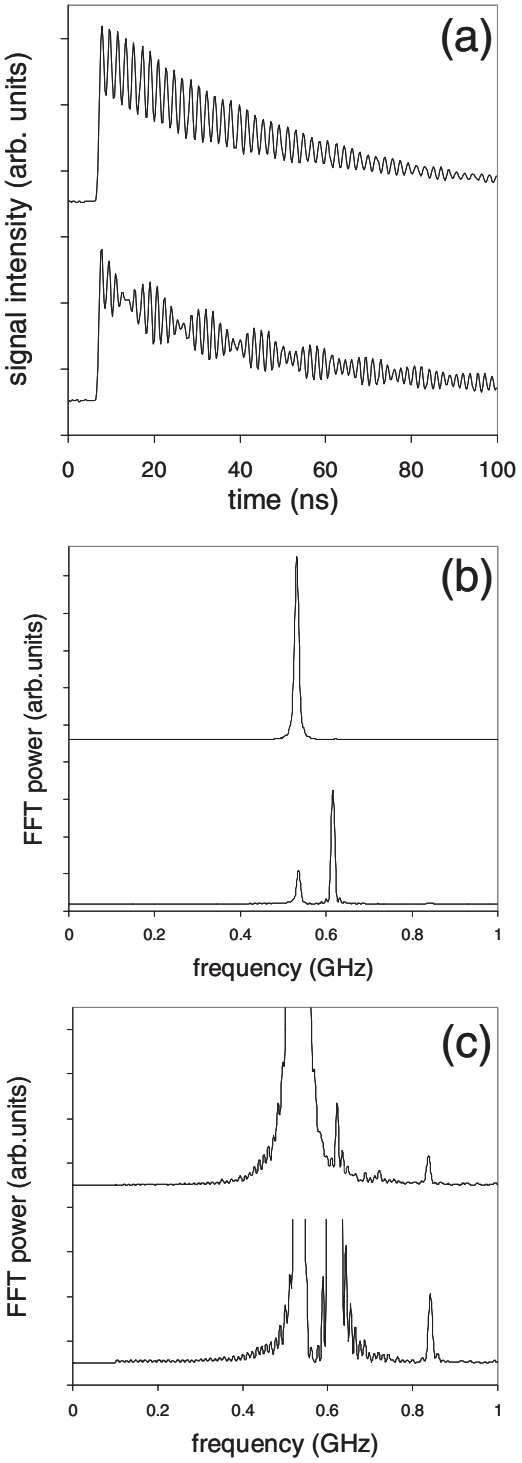

FIG. 3. (a) Signal wave forms, (b) corresponding FFT spectra, and (c) spectra magnified by a factor of 400 compared to (b) for excitation grating wave vector perpendicular to Cu lines. The wave number was set to 0.91 (top) and 1.16 μm^{-1} (bottom: the corresponding reduced wave number is 0.93 μm^{-1}).

however, that this is not a true band gap in the density of states as the dispersion curve of the second mode bends down and overlaps with the band gap in frequency. A much larger band gap is formed inside the Brillouin zone. The signal wave forms corresponding to the band gaps are presented in Fig. 5. The small separation between the modes at the zone boundary results in the low-frequency beat pattern in the wave form. Another noticeable feature of the wave forms is a slow decay of the acoustic oscillations compared to the propagation along the Cu lines. The reason for this is that at the band gap the group velocity is zero and thus the "walk out" of the wave packets does not contribute to the oscillation decay. Note that the transient grating technique benefits from this phenomenon in that the precision of the acoustic frequency measurements is enhanced in the vicinity of band gaps.

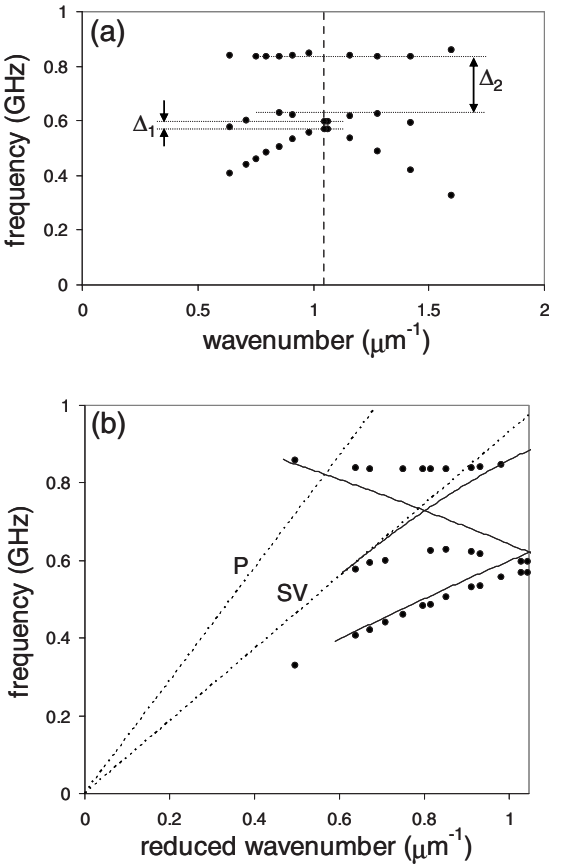

FIG. 4. Measured dispersion curves (solid circles) for surface acoustic modes with wave vector perpendicular to Cu lines plotted (a) vs the excitation grating wave number and (b) vs the reduced wave number. The values of the band gaps are $\Delta_1 = 28$ MHz and $\Delta_2 = 207$ MHz. Vertical dashed line in (a) marks the Brillouin-zone boundary. Solid lines in (b) correspond to measured dispersion curves of the acoustic modes propagating parallel to Cu lines from Fig. 2 replotted vs the reduced wave number. Dotted lines correspond to bulk acoustic waves in Si propagating parallel to the surface in the ⟨011⟩ direction: longitudinal (P) and vertically polarized transverse (SV).

In order to elucidate the origin of the band gap inside the Brillouin zone, dispersion curves for acoustic wave vector parallel to the copper lines from Fig. 2 are replotted in Fig. 4(b) versus the reduced wave number. It is apparent that the band gap arises as a result of the "avoided crossing" of the Sezawa and the zone-folded Rayleigh modes.

Figure 6 presents dispersion curves for a similar structure with 4 μm period. This structure was identical to that stud-

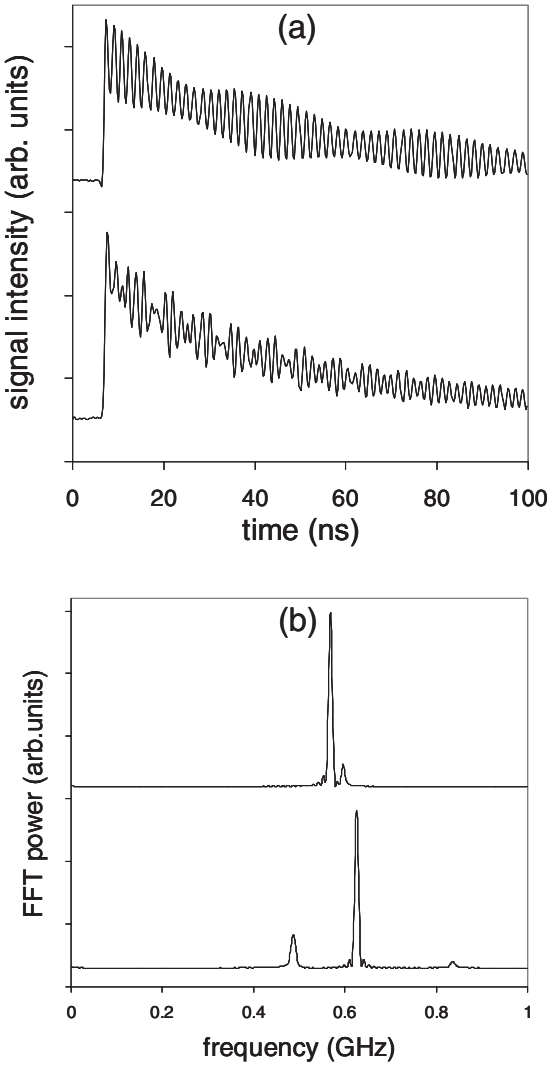

FIG. 5. (a) Signal wave forms and (b) corresponding FFT spectra at the band gaps formed at the Brillouin-zone boundary (top) and inside the Brillouin zone (bottom). The wave-number values are 1.050 (top: 0.3% off the exact value of k_B) and 1.28 μm^{-1} (bottom: the reduced wave number 0.82 μm^{-1}).

ied in Ref. 11, with the exception of the fact that no additional metal coating was used. Again, we see a very small band gap at the Brillouin-zone boundary and a large band gap inside the Brillouin zone. Here, the "avoided crossing" nature of the large band gap is even more evident from the shape of the dispersion curves. The data suggest that the band gap is indirect, i.e., the maximum of the second mode dispersion and the minimum of the third mode are shifted with respect to each other on the wave-number axis.

A comparison of the dispersion curves in Fig. 6 with the results reported in Ref. 11 indicates that the stopband reported in that work most definitely was the large "Rayleigh-Sezawa" band gap. The smaller band gap at the Brillouin-zone boundary would not have been detected in that work due to the limited measurement resolution.

It should be noted that the formation of band gaps inside the Brillouin zone along with those at the zone boundary is a known phenomenon that has been previously observed on

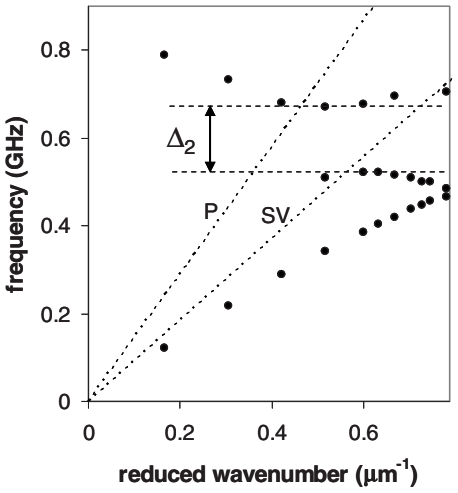

FIG. 6. Dispersion curves (solid circles) measured on a Cu line array with 4 μm period plotted vs the reduced wave number. Dotted lines correspond to bulk acoustic waves in Si: longitudinal (P) and vertically polarized transverse (SV).

silicon samples with a periodic surface profile.[3–5] In that work, band gaps inside the Brillouin zone were ascribed to hybridization and avoided crossing of the Rayleigh wave with the "longitudinal resonance" (i.e., a pseudosurface wave whose velocity is close to that of the longitudinal bulk wave propagating along the surface[2]). For a film-substrate structure one would naturally expect the formation of the Rayleigh-Sezawa band gap inside the zone. What was not expected was the relative width of the band gaps. Why is the Rayleigh-Sezawa band gap so much larger than the Rayleigh band gap at the zone boundary? While numerical calculation of the surface modes would be needed for a comprehensive analysis, the following qualitative explanation is offered as a food for thought.

C. Structure of eigenmodes at band gaps

Let us consider the limit of a weak periodic perturbation (as it would be the case if the embedded Cu lines were very thin). Vertical surface displacement in an acoustic eigenmode characterized by the frequency ω and reduced wave vector k_r can be represented by a superposition of Bloch harmonics,

$$u_z = \sum_{n=-\infty}^{\infty} A_n \exp\left[i\left(k_r + \frac{2\pi n}{d} \right) x - i\omega t \right], \qquad (1)$$

where d is the structure period. In the limit of weak periodicity, eigenmodes closely resemble either Rayleigh or Sezawa waves of the nonperturbed structure, and thus normally only one term in the sum will be significantly nonzero. At the band gaps, however, there will be two significant terms representing counter-propagating waves. At the Brillouin-zone boundary eigenmodes consist of counter-propagating Rayleigh waves with wave number $k_B = \pi/d$. If we place the coordinate origin $x=0$ at a symmetry plane of the structure, for example, at the middle of a copper line, the displacement pattern in the eigenmodes should be either symmetric or antisymmetric. This requirement yields two

standing waves: a symmetric mode with maxima on copper lines and an antisymmetric one with maxima on oxide spaces,

$$u_z^{\text{sym}} \propto \exp(-i\omega_1 t)\cos\left(\frac{\pi x}{d}\right)$$

$$u_z^{\text{asym}} \propto \exp(-i\omega_2 t)\sin\left(\frac{\pi x}{d}\right). \quad (2)$$

One might think that this standing wave pattern leads to a straightforward explanation of the nature of the band gap: the biggest contrast between the properties of Cu and SiO_2 is in their density; the mode with the maximum of the surface displacement on Cu has a larger "effective mass," hence its frequency should be lower.

However, this is not exactly what happens: In SAWs, particle trajectories are elliptical,[17] and thus the oscillations of the horizontal component of the displacement are shifted by $\pi/2$ with respect to the vertical component. In the Rayleigh wave propagating from left to right the motion is counterclockwise[17] while in the wave propagating in the opposite direction it is clockwise, and thus a "true" standing wave with a complete cancellation of motion is not formed. In a normal mode with the node of the vertical displacement component on Cu, the node of the horizontal component will be on SiO_2. Thus neither of the eigemodes has its displacement field mostly concentrated either on Cu or on SiO_2. As a result the frequency gap is not as large as it could be if the normal modes possessed "true" nodes.

Now what is so different about the Rayleigh-Sezawa band gap? In a Sezawa wave the direction of the surface motion is opposite to that in a Rayleigh wave, i.e., it is clockwise for the wave propagating left to right.[17] Therefore, if Rayleigh and Sezawa waves propagate in opposite directions, the direction of the surface motion in both waves will be the same. Thus a normal mode constructed of the counter-propagating Rayleigh and Sezawa waves will have "true" nodes where surface motion will be almost canceled ("almost" because the exact shape of the polarization ellipses in the two modes does not have to be the same).

Let us consider the structure of the eigenmodes at the Rayleigh-Sezawa band gap at the reduced wave number $k_r = k_{\text{RS}}$ in some more details. In the limit of small periodicity, there will be, again, only two significantly nonzero terms in Eq. (1), corresponding to a Sezawa wave at $k = k_{\text{RS}}$ and a Rayleigh wave at $k = k_{\text{RS}} - 2\pi/d$,

$$u_z = A\,\exp(-i\omega t + ik_{\text{RS}}x) + B\,\exp\left[-i\omega t + i\left(k_{\text{RS}} - \frac{2\pi}{d}\right)x\right]. \quad (3)$$

Note that in contrast to the situation at the Brillouin-zone boundary, an eigenmode is not symmetric with respect to the plane $x=0$; rather, symmetry transformation $x^* = -x$ transforms it into an eigenmode with an opposite reduced wave number $k_r = -k_{\text{RS}}$. It can be shown based on the fact that an inversion of either x or t yields an eigenmode with the opposite k_r that if A is real (which can always be assumed without loss of generality), then B is also real. Thus if two terms in Eq. (3) have equal amplitudes then the displacement in the two normal modes will be given by

$$u_z^{(1)} \propto \exp\left[-i\omega_1 t + i\left(k_{\text{RS}} - \frac{\pi}{d}\right)x\right]\cos\left(\frac{\pi x}{d}\right),$$

$$u_z^{(2)} \propto \exp\left[-i\omega_2 t + i\left(k_{\text{RS}} - \frac{\pi}{d}\right)x\right]\sin\left(\frac{\pi x}{d}\right). \quad (4)$$

These are not standing waves, yet they possess nodes with zero displacement either at the center of the Cu lines or at SiO_2 spaces. In reality, the amplitudes do not have to be equal and thus the field cancellation at the "nodes" will be only partial. What is important, however, is that since the surface motion in both Rayleigh and Sezawa waves is clockwise, the horizontal displacement component will have the structure similar to that of the vertical component with the nodes at the same locations. Thus one would expect that in one of the eigenmodes the displacement field is mostly concentrated on the Cu lines and in the other mode on the SiO_2 spaces, resulting in a large band gap.

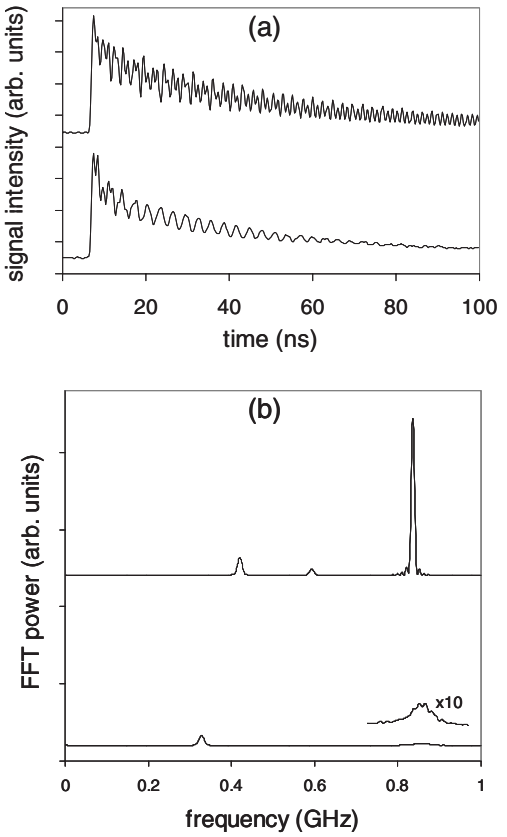

FIG. 7. Brekhovskikh attenuation: (a) Signal wave forms and (b) corresponding FFT spectra measured at wave numbers 1.42 (top) and 1.60 μm^{-1} (bottom). Corresponding reduced wave numbers are 0.67 and 0.50 μm^{-1}, respectively. Inset in (b) shows the weak third mode peak magnified by a factor of 10.

D. Brekhovskikh attenuation

Figure 7 illustrates another interesting effect observed in

this experiment: a dramatic increase in the attenuation of the third mode at the largest excitation wave number. As has been mentioned earlier, when the wave number exceeds k_B, initially the second mode becomes dominant and beyond the Rayleigh-Sezawa band gap the third mode becomes dominant, as can be seen from the top spectrum in Fig. 7. This behavior is consistent with the "avoided crossing" nature of the band gap: Closer to the zone boundary the second mode resembles Rayleigh wave and is excited more efficiently while at larger wave numbers (that correspond to smaller reduced wave numbers) the second mode becomes closer in character to Sezawa wave and the third mode to Rayleigh wave.

When the wave number is increased further, the third mode undergoes a sudden dramatic increase in attenuation as can be seen from the bottom traces in Fig. 7: The high-frequency oscillations in the wave form and the corresponding peak in the spectrum all but disappear. However, a closer examination of the wave form reveals that the high-frequency mode still exists and even has about the same amplitude at the onset of the wave form, but decays within a few oscillation periods. The width of the spectral peak is 60 MHz which yields a decay time of ~5 ns.

It is known that periodicity creates a specific attenuation mechanism for SAWs originally proposed by Brekhovskikh.[19] When SAW dispersion curve becomes zone folded due to periodicity and its "phase velocity" ω/k_r exceeds the phase velocity of bulk waves, SAWs become attenuated via radiation of bulk waves into the substrate.[2,19] Thus modes located above the SV line in Fig. 4(b) should be attenuated via the Brekhovskikh mechanism. They are referred to as "leaky" or "pseudosurface" modes to distinguish them from true surface modes located below the SV line.[2,4,5]

However, the sharp increase in attenuation illustrated in Fig. 7 is not caused by crossing the SV threshold. Indeed, the top wave form corresponds to the reduced wave number 0.67 μm^{-1} and thus the third mode is located well above the transverse threshold. Yet, this mode is rather long lived: The oscillations do not undergo any visible attenuation within the time window of the measurements and thus the decay time exceeds 100 ns. The bottom wave form corresponds to the reduced wave number 0.50 μm^{-1} and thus the third mode is located above the longitudinal threshold labeled "P" in Fig. 4(b). Thus the attenuation increase is most likely caused by radiation of longitudinal waves into the substrate.

A similarly sharp increase in attenuation observed on the sample with 4 μm period is shown in Fig. 8. It occurs at a different wave number (and at a different reduced wave number) which, again, corresponds to the crossing of the longitudinal threshold by the dispersion curve of the third mode. The fact that such a strong effect takes place at the longitudinal threshold and not at the transverse threshold presents an interesting question for further studies.

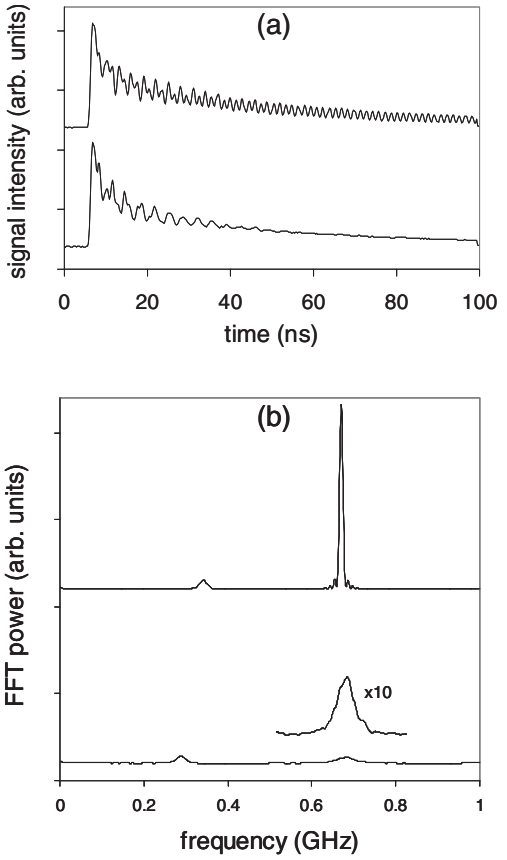

FIG. 8. Brekhovskikh attenuation in the structure with 4 μm period: (a) Signal wave forms and (b) corresponding FFT spectra measured at wave numbers 1.15 (top) and 1.27 μm^{-1} (bottom). Corresponding reduced wave numbers are 0.52 and 0.42 μm^{-1}, respectively. Inset in (b) shows the weak third mode peak magnified by a factor of 10.

IV. CONCLUSION

Transient grating measurements of surface acoustic modes on a periodic array of copper/SiO2 lines on silicon uncovered two interesting phenomena. First, it was found that the avoided crossing of the Rayleigh and Sezawa modes of the film/substrate structure yields a band gap inside the Brillouin zone. This Rayleigh-Sezawa band gap turned out to be much larger than the Rayleigh mode band gap formed at the Brillouin-zone boundary. This finding could be useful in engineering phononic band gap structures for SAWs. The qualitative analysis indicated that the observed behavior stems from the basic properties of the surface modes and thus should be a common occurrence in periodic film/substrate structures. Second, very strong periodicity-induced attenuation was observed above the longitudinal threshold rather than above the transverse threshold. The author hopes that reported findings will stimulate further studies of surface acoustic modes in patterned thin films.

ACKNOWLEDGMENTS

The author would like to thank O. B. Wright for the stimulating exchange of ideas and critical reading of the manuscript. Discussions with A. G. Every are also greatly appreciated.

*Present address: Laboratoire d'Acoustique, Université du Maine, 72085 Le Mans, France

[1] M. Sigalas, M. S. Kushwaha, and E. N. Economou, Z. Kristallogr. **220**, 765 (2005).

[2] N. E. Glass and A. A. Maradudin, J. Appl. Phys. **54**, 796 (1983).

[3] J. R. Dutcher, S. Lee, B. Hillebrands, G. J. McLaughlin, B. G. Nickel, and G. I. Stegeman, Phys. Rev. Lett. **68**, 2464 (1992).

[4] L. Giovannini, F. Nizzoli, and A. M. Marvin, Phys. Rev. Lett. **69**, 1572 (1992).

[5] S. Lee, L. Giovannini, J. R. Dutcher, F. Nizzoli, G. I. Stegeman, A. M. Marvin, Z. Wang, J. D. Ross, A. Amoddeo, and L. S. Caputi, Phys. Rev. B **49**, 2273 (1994).

[6] L. Dhar and J. A. Rogers, Appl. Phys. Lett. **77**, 1402 (2000).

[7] S. Benchabane, A. Khelif, J.-Y. Rauch, L. Robert, and V. Laude, Phys. Rev. E **73**, 065601(R) (2006).

[8] B. Djafari-Rouhani, A. A. Maradudin, and R. F. Wallis, Phys. Rev. B **29**, 6454 (1984).

[9] Y. Tanaka and S. I. Tamura, Phys. Rev. B **58**, 7958 (1998).

[10] G. A. Antonelli, H. J. Maris, S. G. Malhotra, and J. M. E. Harper, J. Appl. Phys. **91**, 3261 (2002).

[11] D. M. Profunser, O. B. Wright, and O. Matsuda, Phys. Rev. Lett. **97**, 055502 (2006).

[12] B. Bonello, C. Charles, and F. Ganot, Ultrasonics **44**, e1259 (2006).

[13] C. Diebold and R. Stoner, in *Handbook of Silicon Semiconductor Metrology*, edited by A. C. Diebold (Dekker, New York, 2001), p. 197; M. Gostein, M. Banet, M. Joffe, A. A. Maznev, R. Sacco, J. Rogers, and K. A. Nelson, *Handbook of Silicon Semiconductor Metrology* (Ref. 13(a)), p. 167.

[14] J. A. Rogers, A. A. Maznev, M. J. Banet, and K. A. Nelson, Annu. Rev. Mater. Sci. **30**, 117 (2000).

[15] A. A. Maznev, K. A. Nelson, and J. A. Rogers, Opt. Lett. **23**, 1319 (1998).

[16] A. A. Maznev, A. Mazurenko, L. Zhuoyun, and M. Gostein, Rev. Sci. Instrum. **74**, 667 (2003).

[17] G. W. Farnell and E. L. Adler, in *Physical Acoustics: Principles and Methods*, edited by W. P. Mason and R. N. Thurston (Academic, New York, 1972), Vol. 9, p. 35.

[18] Equations for calculating effective elastic constants of a periodic layered structure can be found in M. Grimsditch, Phys. Rev. B **31**, 6818 (1985); Elastic constants of chemical vapor deposited SiO2 were taken from J.-H. Zhao, T. Ryan, P. S. Ho, A. J. McKerrow, and W.-Y. Shih, J. Appl. Phys. **85**, 6421 (1999); elastic constants of polycrystalline Cu were obtained from G. Simmons and H. Wang, *Single Crystal Elastic Constants and Calculated Aggregate Properties: A Handbook* (MIT, Cambridge, 1971).

[19] L. M. Brekhovskikh, Sov. Phys. Acoust. **5**, 288 (1960).